EXPERIMENTAL AND THEORETICAL STUDIES OF HELICOPTER ROTOR–FUSELAGE INTERACTION*

N. Bettschart, A. Desopper, R. Hanotel and R. Larguier
Office National d'Etudes et de Recherches Aérospatiales (ONERA)
Châtillon, France

Abstract

Experimental and theoretical studies are presently under development at ONERA on the helicopter rotor–fuselage interactional aerodynamics.

From the experimental point of view, a test was conducted in the ONERA S2 Chalais subsonic wind tunnel to measure the unsteady velocity field around a Eurocopter–France powered helicopter model (Dauphin 365, 1/7.7 scale) in forward flight (μ = 0.2). The unsteady measurements were performed with a three components Laser Doppler Velocimeter.

From the theoretical point of view, an iterative coupling method has been developed for rotor–fuselage calculations. This method is based on a panel method (source and doublet singularities) for the fuselage and on a lifting line theory for the rotor. These two codes are coupled in an iterative approach through an azimuth marching technique.

The experimental results are analyzed and comparisons between experimental and computed results are presented for the ONERA tests and also for tests performed by the US Army Langley. These comparisons show that the fuselage effects have to be taken into account in particular for the rotor wake geometry and for the flow conditions on the inboard part of the rotor disk.

I. Introduction

Helicopters in operation are immersed in a highly complex three–dimensional and unsteady flow field generated principally by the main rotor. Aerodynamic interactions occur between the fuselage, the rotor and the rotor wake. These could have a strong influence on the performance, handling qualities and vibrations of helicopters. Not all these interactions mechanisms are fully understood, causing difficulties to obtain efficient analytic models. Moreover wind tunnel aerodynamic measurements on a helicopter powered model are very time consuming (therefore costly) and require sophisticated equipments.

At the Aerodynamics Department of ONERA, studies on the helicopter rotor–fuselage interactional aerodynamics have been undertaken in order to have a better understanding of the phenomena involved as well as to develop and to validate accurate computational methods. These studies extend the aerodynamic investigations performed at ONERA for several years on isolated helicopter rotor and isolated helicopter fuselage.

The experimental part of the present study consisted in the measurement of the unsteady velocity field around a powered helicopter model. The test was conducted in the ONERA S2 Chalais subsonic wind tunnel and the helicopter model was a 1/7.7–scale Dauphin designed by Eurocopter–France. A three directional Laser Doppler Velocimeter (LDV) was used to perform unsteady velocity field measurements in two planes perpendicular to the free–stream direction.

An iterative coupling computational method for rotor–fuselage configurations is under development. This method is based on a fuselage code developed at ONERA (panel method with source and doublet singularities) and a lifting line rotor code with a vortex wake modelization developed at Eurocopter–France. The iterative coupling between these two codes is based on a quasi steady approach and is achieved by an azimuth marching technique.

Calculations were performed on two configurations, the realistic Dauphin model and a simplified helicopter model tested at NASA Langley Research Center. The comparisons between calculation and experiment show that the fuselage effects have to be taken into account to improve the predictions, in particular for the flow characteristics on the inboard part of the rotor disk and for the rotor wake geometry.

II. Theoretical methods

Isolated fuselage code

A low order panel method, based on the hypothesis of a 3–D inviscid steady incompressible flow, was developed at ONERA [1].

* This research was partially supported by the French Ministry of Defence and by the EEC within the BRITE EURAM SCIA programme.

Potential flow is assumed and the total velocity is the sum of the undisturbed free–stream velocity and a perturbation velocity due to the presence of the body (fuselage) in the flow. The total potential is a solution of the Laplace equation with the following two classical boundary conditions: a slip condition on the body surface and a vanishing perturbation velocity at an infinite distance from the body. This initial Neumann problem is converted into an inner Dirichlet formulation with a fixed potential inside the body. The fuselage is discretized by a set of plane quadrilateral panels of constant source and doublet strength. The sources intensities are explicitly given by the normal velocity on the body surface. The doublets and the potential are linked by a Green's integral formulation. The linear system derived from the discretized equations is solved by a Lower–Upper technique (LU) with optimized asynchronous input/output. In this formulation the elements of the influence matrix depend only on the body geometry. The perturbation velocity on the body is computed by a 2nd order finite difference scheme. Using Green's vector identity, the velocity field is then determined everywhere. Calculations with a prescribed fuselage wake can also be performed, but for the present calculations no fuselage wake is considered (see figure 1).

Isolated rotor code

The lifting line method used for the description of the rotor and its wake was developed by Eurocopter–France (METAR code) [2]. The actual continuous circulation distribution along the blade span is discretized by a step function (see figure 2). The rotor wake is modeled by a lattice of longitudinal and radial linear vortex segments emitted by the blades with the conventional prescribed helical rotor wake geometry (see figure 3). The vorticity strength of a segment in the wake is related to the discretized circulation variation computed at the time step (azimuthal position of the rotor) and at the span position where this segment left the blade. The rotor aerodynamic solution is carried out by an iterative process initialized by the Meijer–Drees induced velocity: the lift is obtained through 2–D experimental airfoil tables with the computed local angle of incidence and Mach number and the circulation is derived from the Joukowski law. The new induced velocity distribution at the rotor control points is given by the Biot and Savart formula. The convergence criterion is based on the induced velocity variation between two successive iterations. For the present calculations, the blades are discretized into ten segments and a complete revolution in 24 azimuthal steps ($\Delta\psi = 15°$). The rotor wake discretization includes three rotor revolutions.

Coupled method

A computational method for rotor–fuselage configurations is under development at ONERA by coupling the isolated fuselage code and the METAR code presented above.

This iterative coupling procedure is based on a quasi steady approach and was achieved by an azimuth marching technique (see figure 4). For a spatial point attached to the body, the flow has a periodicity equal to the blade passing period. In order to reduce the computational resources (time and storage), it is not necessary to consider all the azimuthal positions needed to describe a whole rotor revolution. Only those included in the blade–to–blade interval are actually computed (the azimuthal increment must be chosen so that the blade–to–blade interval is a multiple of it).

The process is initialized by a Mejer Drees inflow computation. The isolated fuselage influence is taken into account, at the rotor control points, for a rotor calculation. An iterative loop on the azimuthal rotor position is then started. For each azimuth (or time step), the velocities induced by the rotor and its wake are computed at the fuselage collocation points by the Biot and Savart law. The fuselage singularities strengths are then evaluated by solving the linear system for which the new boundary conditions are taken into account on the fuselage surface. During this process, only the right hand side of the linear system is modified. Therefore the influence matrix is inverted once and stored. The new fuselage singularity distribution is then used to compute the velocities in the rotor wake in order to distort its geometry. They are also computed on the blades for the rotor calculation at the next time step. The fuselage influence is therefore supposed to be constant between two time steps. Furthermore, the rotor wake is deformed only by the velocity field induced by the fuselage. The convergence of this procedure is obtained after two or three rotor revolutions.

III. Comparison between experimental and theoretical results

Calculations were performed on experimental configurations studied at the ONERA and at the NASA Langley Research Center from which we have also experimental data.

NASA configurations

Experimental investigations were conducted in the 14–by 22–Foot Subsonic Tunnel at the NASA Langley Research Center. Different sets of data, coming from two distinct investigations, were used for the present correlations.

The first study was dedicated to the measurement of the time–average fuselage surface pressure of a helicopter powered model [3]. The rotor system used was a 3.15–meter diameter, four–bladed rotor with a fully articulated hub. The ROBIN (ROtor Body INterference) fuselage is an analytic surface which can be determined easily using its mathematical definition given in reference [3]. One hundred and seventy six orifices were located on different fuselage cross sections. Averaged pressure measurements were performed at hover and at various advance ratio for a range of thrusts. Isolated fuselage configurations were also tested.

Calculated and experimental pressure distribution on the lateral lines z/R = 0 are compared for an isolated fuselage (Figure 5, $\alpha_{fuselage}$ = 0°) and for a rotor–fuselage configuration (Figure 6, $\alpha_{fuselage}$ = –1°, C_T = 0.0062, μ = 0.2). For these calculations, the fuselage was discretized with 2756 panels. The rotor–fuselage configuration was computed only by taking into account a mean rotor downwash (i.e. that the fuselage computation is performed by taken into account only the mean induced velocities without any rotor wake deformation). Agreement between experimental and computed results is fairly good in both cases. For the complete configuration, the mean rotor downwash improves the theoretical prediction: the dissymmetry between the fuselage left and right sides is correctly described. However, computation with a mean rotor downwash can only give reasonable results if the aerodynamic interaction between the rotor wake and the fuselage is weak (i.e. for relatively high advance ratio and/or for fuselage regions not directly exposed to the rotor wake). When strong interactions occur (see figure 6, x/R > 1.2 for example), a fully coupled calculation is necessary.

The second experimental investigation consisted in the measure of the rotor inflow of a helicopter powered model in forward flight by a Laser Velocimeter technique. Two instantaneous velocity components (vertical and longitudinal to the free–stream direction) were measured, one chord above the plane formed by the blade tip, for three advance ratio (μ = 0.15, 0.23, 0.3) [4]. Only the rectangular blades are considered in the present study. The model system used in this experiment was the 2–Meter Rotor Test System (2MRTS) with the same generic fuselage shape (ROBIN) described above but approximately one and a half smaller. The four–bladed, fully articulated rotor has a diameter of 1.7 m. Further details about the 2MRTS can be found in reference [5].

Figures 7 and 8 present comparisons between the experimental and computed mean and instantaneous vertical induced velocity for μ = 0.3. For this relatively high advance ratio, the mean vertical induced inflow is positive (vertical velocity upwards) on a large portion of the front part of the rotor disk (figure 7). The isolated rotor prediction underestimates this region while the coupled calculation shows a clear improvement with the zero–inflow line moved back to the rotor disk center. However, the coupled calculation overestimates the downstream inflow in the rear part of the disk. This overestimation is certainly due to the inviscid hypothesis of the fuselage code for which the calculated flow remains attached behind the hub fairing, inducing a local vertical velocity field. These results are similar to the ones presented in reference [2] and [6]. Figure 8 shows the instantaneous vertical velocity versus the azimuth for three radial positions (r/R = 0.4, 0.78, 0.98) along the azimuth ψ_m = 180° (front part). Coupled and isolated rotor calculations are in phase with the experiment for the two inner radial locations. The calculations slightly overestimate the peak–to–peak amplitude fluctuations especially at r/R = 0.78 and 0.98. The coupled calculation improves the correlation in particular for the inboard radial positions.

Dauphin configuration

Tests on a powered helicopter model were performed to measure the unsteady velocity field around the fuselage and the rotor using a three–directional Laser Doppler Velocimeter (LDV). The experiments were conducted in the ONERA 3–meter diameter S2 Chalais wind tunnel. The powered model used for this investigation is a very realistic 1/7.7–scale Dauphin 365 (about 1.5 meter long). It was built by Eurocopter–France under fundings from the French Ministry of Defence ("Direction des Recherches et Etudes Techniques"). The rotor system is a 1.5–meter diameter, four–bladed rotor with a 9% thick OA209 airfoil. The rotor blades are rectangular with a constant 0.05–meter chord, a –12° linear twist and a rotating tip speed equal to 100 m/s. The rotor hub is fully articulated and the rotor is controlled by means of a swashplate which determines the collective and cyclic pitch angles.

The Laser Doppler Velocimeter used in this experiment was developed at ONERA [7]. It uses the classical technique of interference fringes between three laser beams produced by two argon laser. Bragg cells in each optical path provides the sign of the velocity component. Cassegrain telescopes collect the light scattered from the particles passing through the sample volume. Three laser doppler signal processors (DISA counters) and a mini–computer are devoted to the acquisition and the processing of the data. Back or forward scattered mode can be used with the whole LDV system mounted on one (or two) very rigid table(s) allowing precise, synchronized and automated displacements along three orthogonal axes. The unsteady velocity measurements were performed in two transversal planes located at x/R = 0 and x/R = 0.42 downstream, relatively to the rotor center, and for the advancing blade side only. Figure 9 shows the LDV measurement planes and the coordinate system. The measurements were performed every 4° in azimuth, which means 90 slots to describe one rotor revolution. The slots had a width of 1° in azimuth (≅ 131 µs) and for each slot the measurements were averaged over 100 samples. Results previously obtained for an isolated rotor can be found in [8] and [9].

The configuration tested corresponds to an advance ratio μ = 0.2 and a simulated mass of 4000 Kg (C_T = 0.0062). Coupled and isolated rotor calculations were performed for this configuration. The 6526–panel mesh of the Dauphin fuselage used for the coupled computations is presented in figure 10.

Figure 11 shows a comparison between the experimental and the computed mean crossflow velocities in the plane x/R = 0. The big swirling structure located at the edge of the rotor disk, which is due to the strong concentration of the blade tip vortices, can be seen on the experimental results, on the coupled and the isolated rotor calculations. However, in both calculations, the "edge vortex" position is lower than in the experiment.

Figures 12 and 13 show in detail the radial evolution of the mean velocities (vertical and radial) for five vertical stations. The differences between the isolated rotor and the coupled calculation are small, except in the regions near the fuselage ($y/R < 0.3$) where the flow is deviated. Nevertheless, the computational results are far to compare with the experimental data; the decrease of the mean vertical velocity with the vertical station is underpredicted in the both calculations. These discrepancies are certainly due to the fact that METAR is a prescribed rotor wake code and that a rotor free wake analysis is required for this kind of configuration. Figure 14 presents the mean vertical velocities in the plane $x/R = 0.42$. A better agreement is obtained than at $x/R = 0$.

The Azimuthal evolutions of the instantaneous velocities are presented in figures 15–18.

The instantaneous vertical velocities for different points located just above the rotor disk in the plane $x/R = 0$ (figure 15), show that outside the rotor disk ($y/R > 1$), the velocity fluctuations are small and the mean value is positive (upwash) while inside the rotor disk ($y/R < 1$) the fluctuations due to the blade passage are much larger and the mean value is negative (downwash). Due to the blade motion (flapping and coning angles), the vertical distance between measurement points and the blade becomes smaller as one moves from the root to the blade tip. This could explain the larger velocity fluctuations for the radial positions $y/R = 0.9$ and 0.8.

However, the shape of these fluctuations seems to point out that other phenomena (as blade vortex interactions) are probably involved. At $y/R = 0.37$ and 0.58, the azimuthal evolution of the vertical velocity has a regular "sawtooth" characteristic due to the blade passage. At $y/R = 0.8$, the sawtooth structure is still found, but the velocity slope between two successive blade passages is inverted. Near the blade tip ($y/R = 0.9$), the velocity evolution suggests very strong aerodynamic interactions between the blades and the rotor wake. For most of these measurements points, which are quite distant from the fuselage, isolated rotor and coupled calculations are very similar. The peak–to–peak amplitude fluctuations and the mean value of the vertical velocity are systematically underpredicted but the computed results are in phase with the experiment.

For isolated rotor calculations, figure 16 shows the influence of the azimuthal step on the instantaneous vertical velocity. The velocity jump corresponding to the blade passage is a little better described with $\Delta\psi = 6°$ than with $\Delta\psi = 15°$.

Figures 17 and 18 present the vertical and radial instantaneous velocities for measurements located at different z/R near the blade root ($y/R = 0.13$) in the plane $x/R = 0.42$. For these points located near the fuselage the differences between the isolated rotor and the coupled calculations are larger. Correlations with the experiment are not very good for the vertical velocities (figure 17): above the rotor disk ($z/R = 0.079$) both calculations are in phase with experiment but the fluctuations amplitude is underpredicted. Below the rotor disk neither the phase nor the amplitude are satisfactory. For the radial velocities (figure 18), the coupled calculation improves the correlation with the experiment.

The wake geometry is strongly modified when the fuselage effect is taken into account in the calculations. Figure 19 shows the intersection between the rotor wake and the measurement plane $x/R = 0$ for a given rotor position (the blade 1 being at $\psi = 105°$). For the helical rotor wake geometry used in the isolated rotor calculation, the intersection points are regularly shifted down. When the fuselage is taken into account (coupled calculation), the rotor wake is moved around the fuselage and its geometry is distorted. This effect is very important in the vicinity of the fuselage which induces upwash and vortex filaments can be moved above the rotor disk. The tip vortex trajectories (figure 20) show the same phenomena.

IV. Conclusions and perspectives

An experimental investigation was conducted using a 3–D Laser Doppler Velocimeter to study the flow around a Dauphin powered helicopter model. The results obtained point up the severe aerodynamic characteristics of a helicopter in forward flight. The LDV technique proved to be a very powerful tool to perform measurements around such complex configurations with moving surfaces.

Calculations were performed for both the NASA Langley and the Dauphin ONERA tests. Comparisons with the experimental results show that the fuselage effects have to be taken into account on the inboard part of the rotor disk and to compute the rotor wake geometry. Reasonably good agreement on the mean and instantaneous velocity field is found with the experiment above the rotor disk. However the influence of the rotor wake on itself seems to be the major effect for the regions located in the rotor wake. This is probably the main reason for the discrepancies observed on the Dauphin calculations, for which detailed measurements are available below the rotor disk.

The present computational method will be improved by a complete free wake rotor approach which appear absolutely necessary. Unsteady pressure predictions including a close vortex–body interaction technique will be performed and compared with the future experimental investigations on the Dauphin powered model. They will be devoted to the steady and unsteady pressure measurements on the fuselage and to the determination of the rotor wake geometry.

References

[1] T.H. LE, J. RYAN, G. FALEMPIN. Wake modeling for helicopter fuselage. 13th European Rotorcraft Forum, Arles, September 1987.

[2] A. DEHONDT, F. TOULMAY. Influence of fuselage on rotor inflow performance and trim. 15th European Rotorcraft Forum, Amsterdam, September 1989.

[3] C.E. FREEMAN, R.E. MINECK. Fuselage surface pressure measurements of a helicopter wind-tunnel model with a 3.15-meter diameter single rotor. NASA Technical Memorandum 80051, March 1979.

[4] J.W. ELLIOTT, S.L. ALTHOFF, R.H. SAILEY. Inflow measurement made with a laser velocimeter on a helicopter model in forward flight. Volumes I, II, III, NASA Technical Memorandum 100541 to 10543, April 1988.

[5] A.E. PHELPS III, J.D. BERRY. Description of U.S. Army small-scale 2-meter rotor test system. NASA Technical Memorandum 87762, February 1987.

[6] D.R. HOAD, S.L. ALTHOFF J.W. ELLIOTT. Aerodynamic study of a hovering rotor. 44th Annual Forum of the American Helicopter Society, Washington D.C., 1988.

[7] A. BOUTIER, E. HAZIZA, D. LEFEBVRE, J. LEFEVRE. New applications of laser velocimetry in ONERA wind tunnels. 10th ICIASF, Saint-Louis, September 1983.

[8] J.M. POURADIER, E. HOROWITZ. Aerodynamic study of a hovering rotor. 6th European Rotorcraft and Powered Lift Aircraft Forum, Bristol 1980.

[9] A. DESOPPER. Rotor wake measurements for a rotor in forward flight. International Conference on Rotorcraft Basic Research, Research Triangle Park, North Carolina, February 1985.

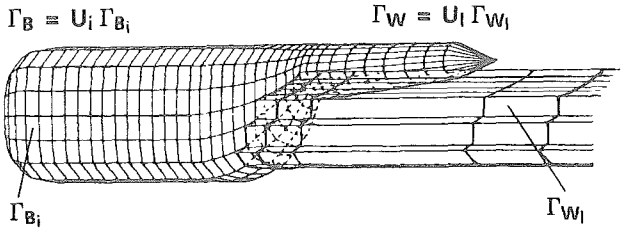

Fig. 1 – Isolated fuselage code.

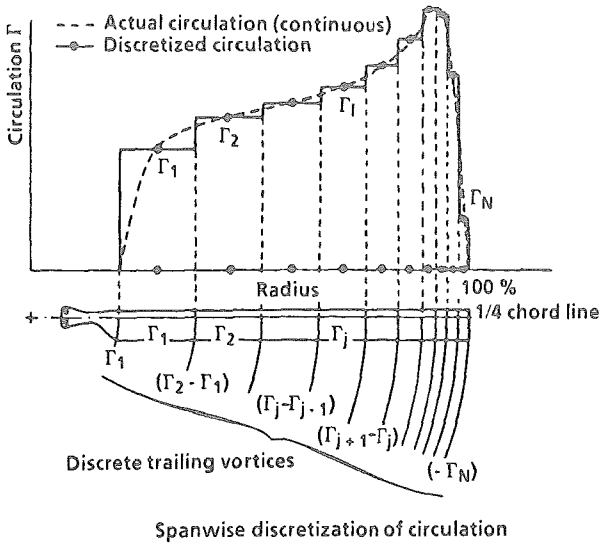

Fig. 2 – Isolated rotor code. Blade circulation discretization.

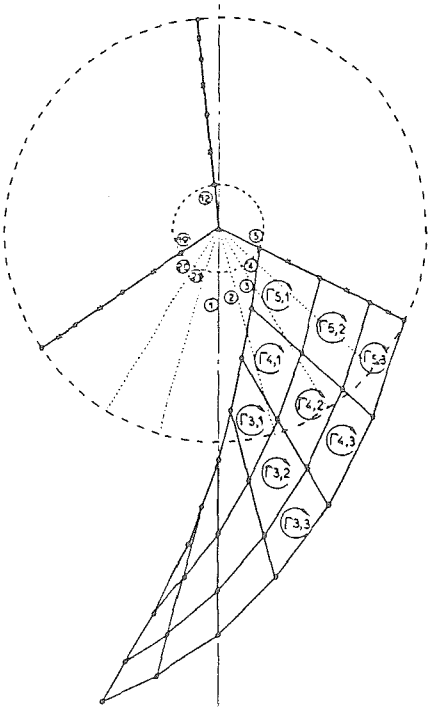

Fig. 3 – Isolated rotor code. Rotor wake modeling.

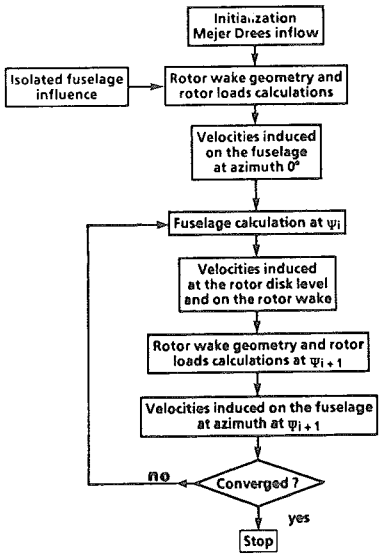

Fig. 4 – Flow chart of the coupled method.

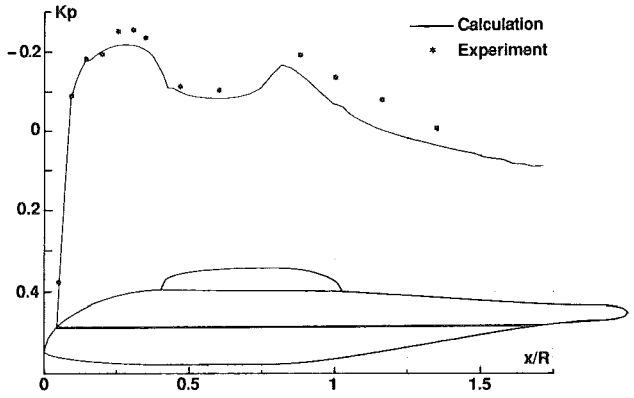

Fig. 5 – Isolated fuselage calculation. Pressure distribution on lateral line z/R = 0, $\alpha_{fuselage} = 0°$.

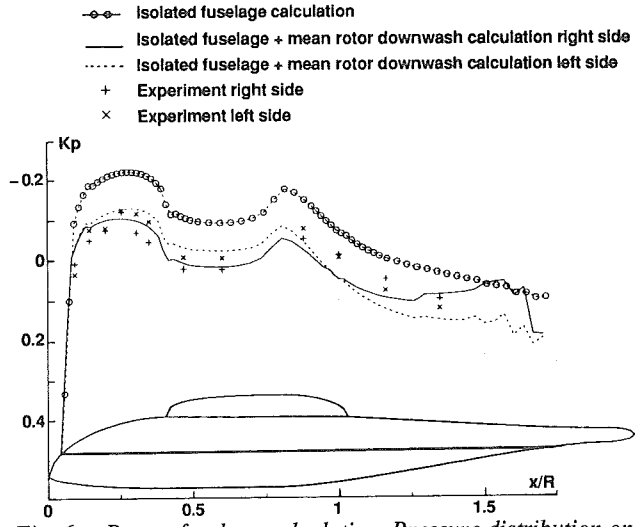

Fig. 6 – Rotor–fuselage calculation. Pressure distribution on lateral lines z/R = 0,
$\alpha_{fuselage} = -1°, \mu = 0.2, C_T = 0.0062$.

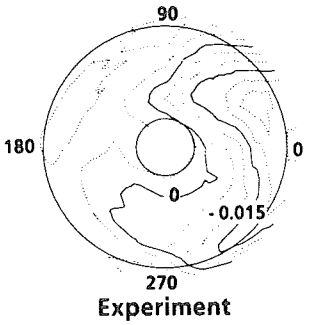

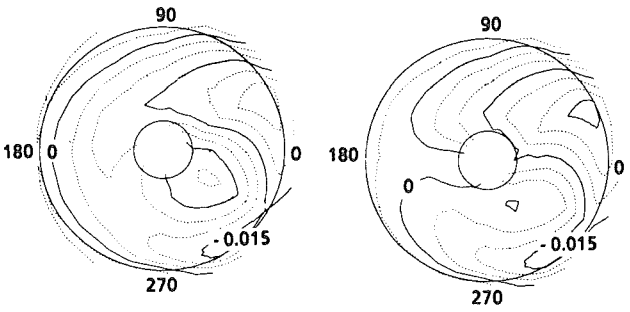

Fig. 7 – Mean vertical velocity ratio distribution.
$\overline{w}/V_{tip}$ (positive up), $\mu = 0.3$.

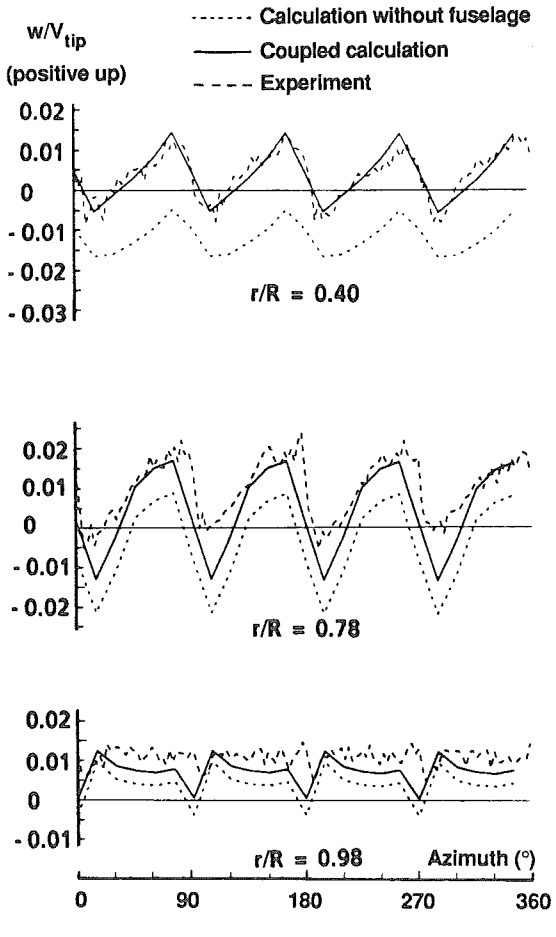

Fig. 8 – Instantaneous vertical velocity ratio.
Measurement azimuth: $\psi_m = 180°, \mu = 0.3$.

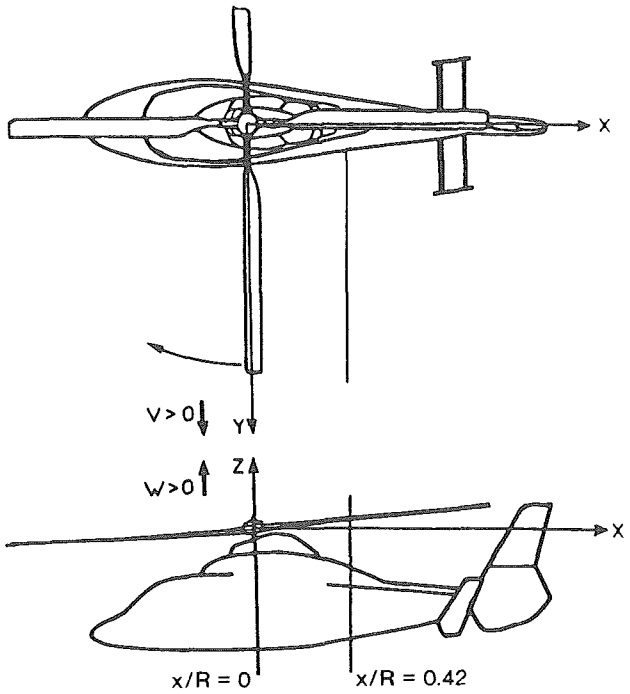

Fig. 9 – Configuration of the LDV measurement planes and coordinate system.

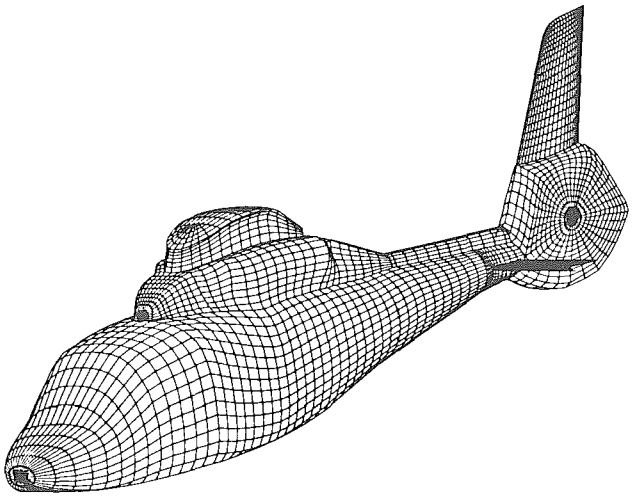

Fig. 10 – Mesh of the Dauphin fuselage.

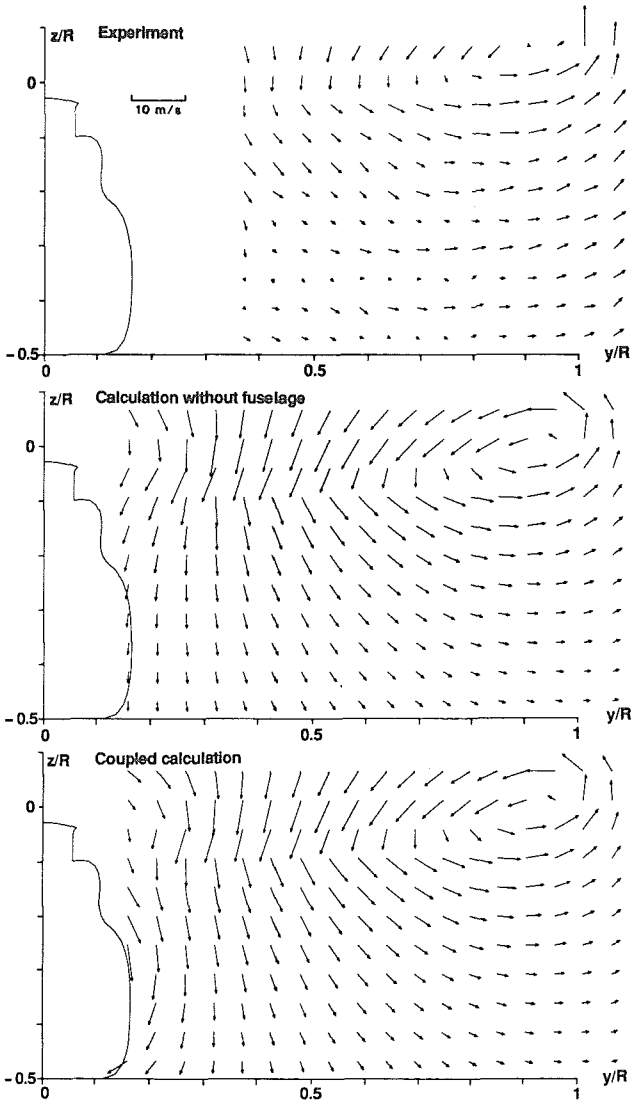

Fig. 11 – Mean velocities crossflow in the plane x/R = 0.

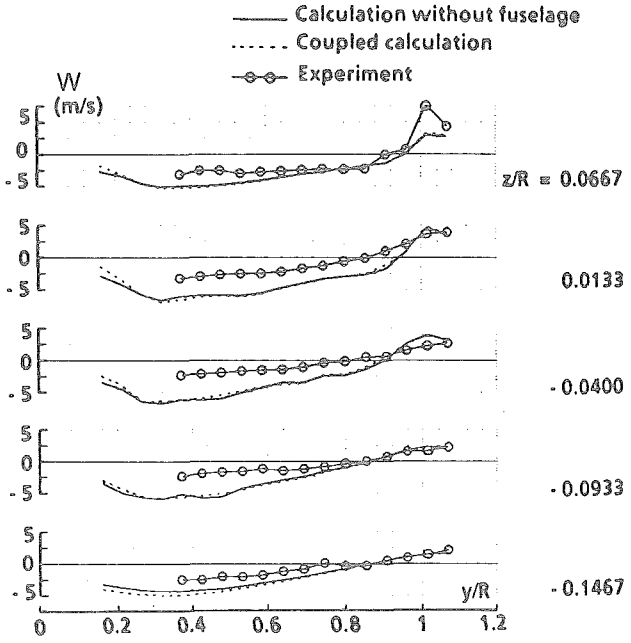

Fig. 12 – Mean vertical velocities: x/R = 0.

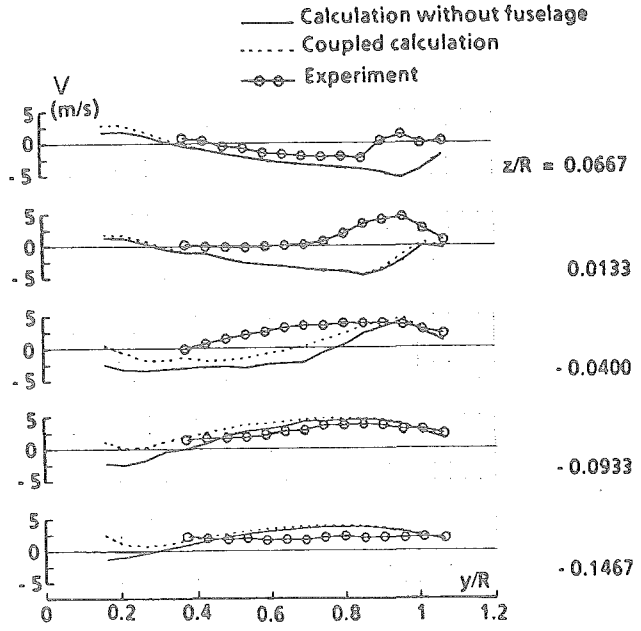

Fig. 13 – Mean radial velocities: x/R = 0.

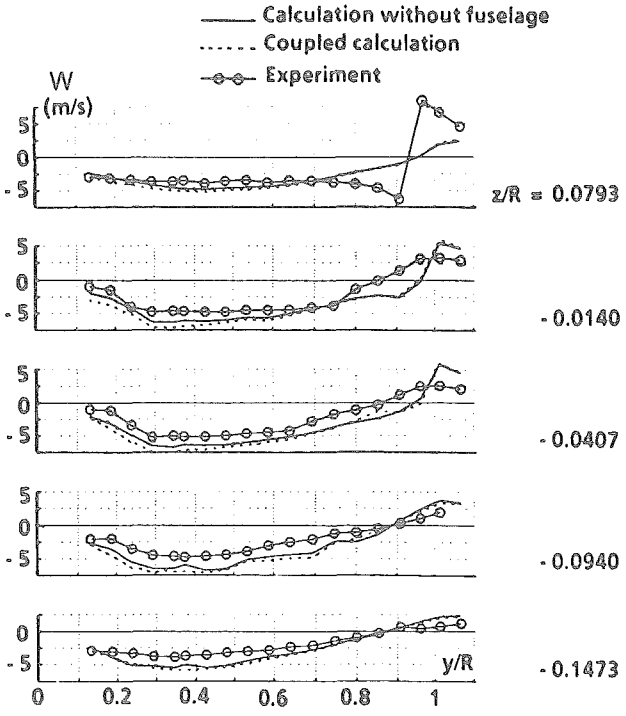

Fig. 14 – Mean vertical velocities: x/R = 0.42.

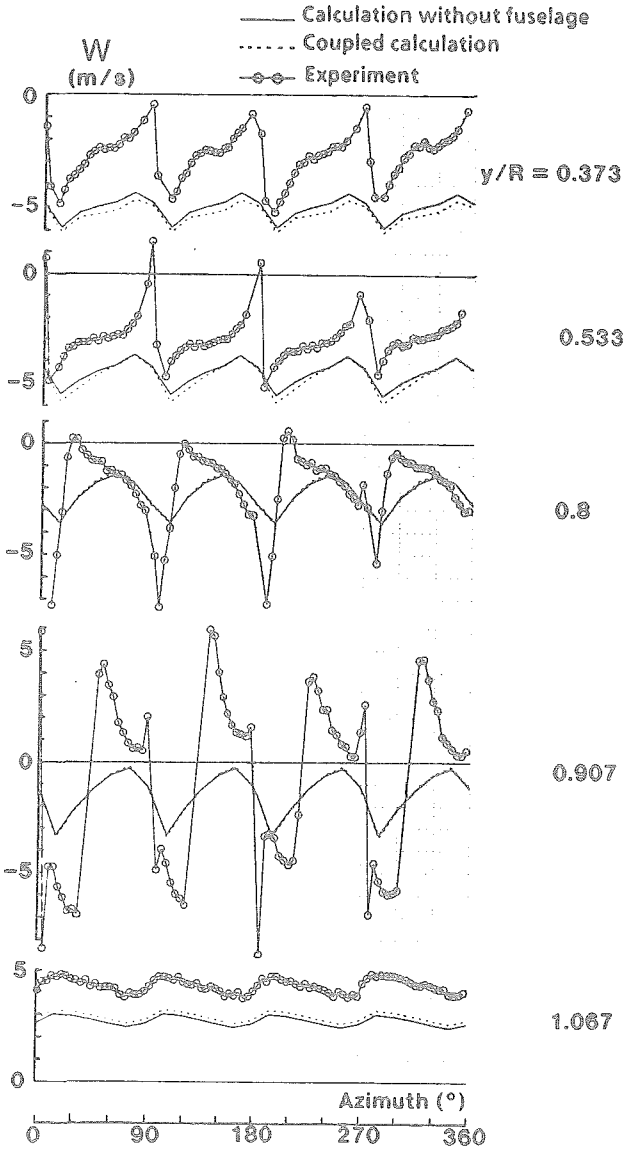

Fig. 15 – Instantaneous vertical velocities: x/R = 0, z/R = 0.066.

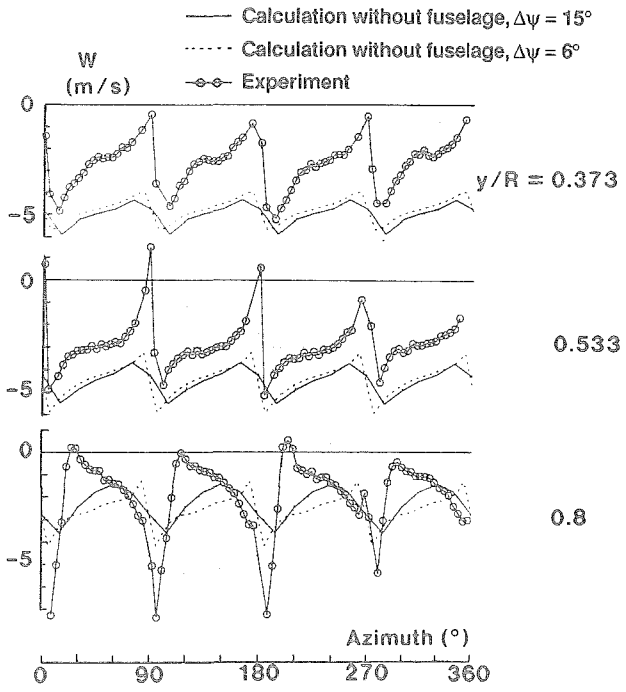

Fig. 16 – Influence of the azimuthal step on the instantaneous vertical velocities, x/R = 0.

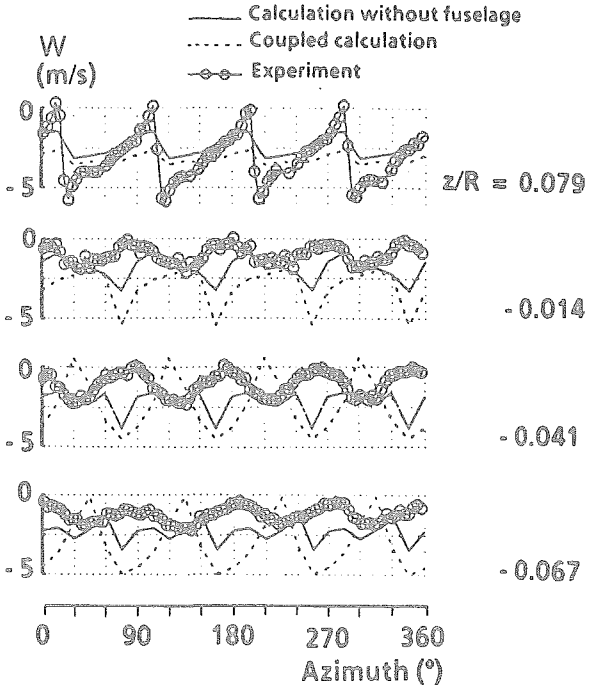

Fig. 17 – Instantaneous vertical velocities: x/R =0.42, y/R = 0.13.

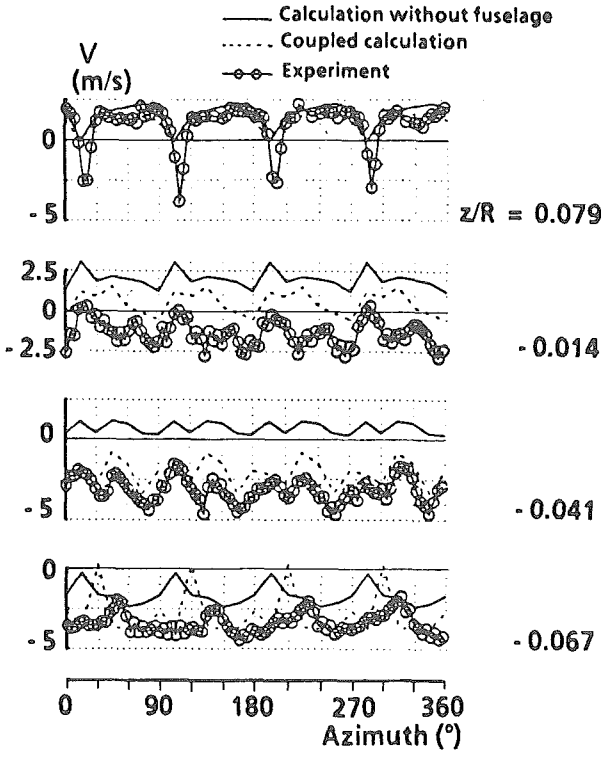

Fig. 18 – Instantaneous radial velocities: x/R = 0.42, y/R = 0.13.

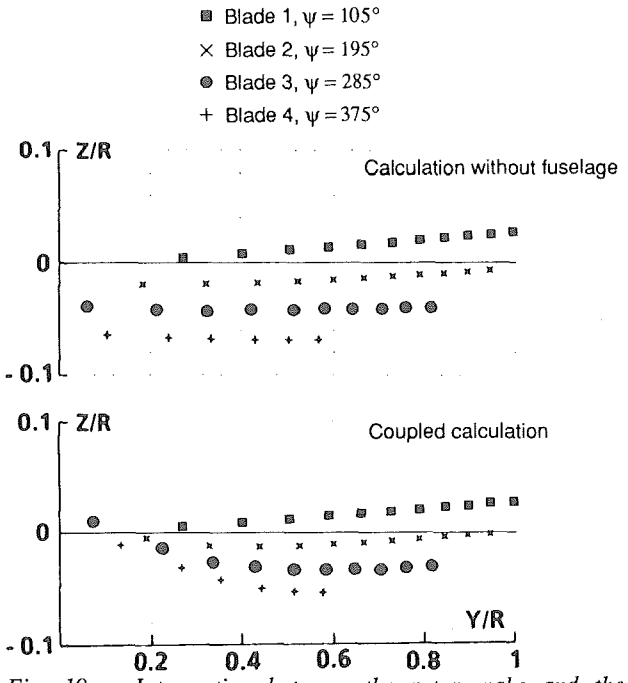

Fig. 19 – Intersection between the rotor wake and the measurement plane x/R = 0.

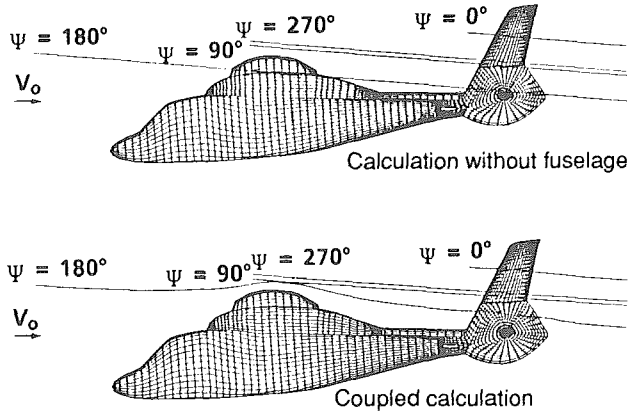

Fig. 20 – Tip vortex trajectories.